

# ON SPECTRAL GAPS IN GRAPHENE IN A WEAK CONSTANT MAGNETIC FIELD

M. H. Brynildsen, H. D. Cornean

Aalborg University, Department of Mathematics, Aalborg, Denmark  
mikkelhb@math.aau.dk, cornean@math.aau.dk

We present a mathematical introduction to a widely used discrete tight-binding model for graphene. We also introduce the “Peierls substitution,” modelling the Hamiltonian of a 2d crystal in a perpendicular uniform magnetic field in this setting. We consider a discrete single-cone Hamiltonian closely related to the (double-cone) graphene Hamiltonian. Finally, we announce in this paper a result concerning an opening of gaps in the spectrum of this single-cone Hamiltonian, when the Peierls phase-factor arises from a weak, but non-zero, external magnetic field. Full proofs will be given elsewhere.

## 1. Introduction

Graphene, carbon atoms arranged in a flat honeycomb lattice, possesses many interesting electronic properties [1, 9]. After the realization of large graphene crystals in the laboratory [10] the interest, theoretical and experimental, has been intense. One of the main features is what physicists call the “relativistic behavior” of electrons in graphene, electrons in graphene can be viewed as massless fermions living in a 2d space, with their dynamics generated by a Weyl Hamiltonian, i.e., a Dirac Hamiltonian with zero rest mass.

We present here a standard analysis of graphene which shows the Weyl fiber, a discrete treatment of graphene which dates back to [13], if not earlier.

We have for some time been interested in the electronic properties of a graphene sheet subjected to a perpendicular uniform magnetic field. We model this situation by multiplying the Hamiltonian integral kernel by unimodular phase factors, this technique is known as “Peierls substitution” [6, 7, 11].

## 2. The Setting and Main Result

### 2.1. A Crystal Structure in the $XY$ -plane

We will now introduce our notation for the set of atom-sites of a two-dimensional crystal lying in the  $XY$ -plane. A crystal structure is constructed by the indefinite periodic repetition of a crystallographic basis<sup>1</sup>. The honeycomb structure of a graphene monolayer is an example of such a crystal structure. More generally, consider a two-dimensional crystal structure embedded in the  $XY$ -plane of  $\mathbb{R}^3$ . The set of primitive vectors  $\{\mathbf{a}, \mathbf{b}\}$ , where we denote  $\mathbf{a} = (\mathbf{a}_1, \mathbf{a}_2)$  and  $\mathbf{b} = (\mathbf{b}_1, \mathbf{b}_2)$ , generates the Bravais lattice:

$$\Gamma = \text{Bravais lattice} := \{\gamma = (\gamma_1, \gamma_2) \in \mathbb{R}^2 : \gamma = m\mathbf{a} + n\mathbf{b}, m, n \in \mathbb{Z}\}. \quad (2.1)$$

A primitive unit cell of  $\Gamma$  is given by

$$\Omega = \text{unit cell} := \left\{ x = (x_1, x_2) \in \mathbb{R}^2 : x = \theta_1\mathbf{a} + \theta_2\mathbf{b}, -\frac{1}{2} < \theta_1, \theta_2 \leq \frac{1}{2} \right\}. \quad (2.2)$$

---

<sup>1</sup>We will use the crystallographic nomenclature to distinguish between a Bravais lattice and a general crystal structure. This nomenclature unfortunately includes the word “basis” for the entity which is being repeated in definitely to generate the crystal.

We choose the order of the primitive vectors such that the ordered set of vectors  $(\mathbf{a}, \mathbf{b}, \hat{z})$  defines a right-handed coordinate system. Then the area of the unit cell is given by  $|\Omega| = |\mathbf{a} \wedge \mathbf{b}| = |\mathbf{a}_1 \mathbf{b}_2 - \mathbf{a}_2 \mathbf{b}_1|$ . In our model  $\mathcal{B}$  contains two vectors:

$$\mathcal{B} = \text{crystallographic basis} = \{\underline{\xi}, \underline{\zeta}\},$$

it is no restriction to put  $\underline{\xi} = 0$ . The crystal structure now has the form

$$\Lambda = \Gamma + \mathcal{B}. \quad (2.3)$$

An element  $x \in \Lambda$  is the position, or site, of an nucleus of an atom in the two-dimensional crystal filling the  $XY$  plane. The reciprocal lattice  $\Gamma^*$  is generated by the primitive vectors  $\{\mathbf{a}^*, \mathbf{b}^*\}$  that satisfies the identities:

$$\mathbf{a} \cdot \mathbf{a}^* = \mathbf{b} \cdot \mathbf{b}^* = 2\pi, \quad \mathbf{a} \cdot \mathbf{b}^* = \mathbf{b} \cdot \mathbf{a}^* = 0, \quad (2.4)$$

where  $v \cdot w$  denotes the euclidean scalar product between vectors  $v, w$  in  $\mathbb{R}^n$ . One can easily see that this fixes  $\{\mathbf{a}^*, \mathbf{b}^*\}$  from  $\{\mathbf{a}, \mathbf{b}\}$ :

$$\mathbf{a}^* = \frac{2\pi}{|\Omega|}(\mathbf{b}_2, -\mathbf{b}_1), \quad \mathbf{b}^* = \frac{2\pi}{|\Omega|}(-\mathbf{a}_2, \mathbf{a}_1). \quad (2.5)$$

The reciprocal lattice is regarded as a subset of  $\mathbb{R}^2$ :

$$\Gamma^* = \text{reciprocal lattice} := \{\gamma^* = (\gamma_1^*, \gamma_2^*) \in \mathbb{R}^2 : \gamma^* = m\mathbf{a}^* + n\mathbf{b}^*, m, n \in \mathbb{Z}\}. \quad (2.6)$$

The first Brillouin zone is the Wigner-Seitz primitive cell of the reciprocal lattice:

$$\Omega^* := \{k = (k_1, k_2) : \|k\| \leq \|k - \gamma^*\|, \text{ for all } \gamma^* \in \Gamma^*\}, \quad (2.7)$$

that is,  $\Omega^*$  is the closure of all the points of  $\mathbb{R}^2$  that are closer to zero than any other point in the reciprocal lattice. Note that

$$|\Omega||\Omega^*| = (2\pi)^2, \quad (2.8)$$

where  $|S|$  denotes the Lebesgue measure of a Borel set  $S \subset \mathbb{R}^2$ .

We work in a one-electron setting, neglecting electron-electron interactions. Our Hilbert space is  $\ell^2(\Lambda)$ , in which the Kronecker-basis  $\{\delta_x\}_{x \in \Lambda}$ :

$$\delta_x(x') := \begin{cases} 1 & \text{if } x' = x, \\ 0 & \text{if } x' \neq x, \end{cases}$$

is a total orthonormal set. We denote the inner product between two vectors  $\psi, \psi'$  of  $\ell^2(\Lambda)$  by  $\langle \psi, \psi' \rangle$ .

## 2.2. Bloch–Floquet Decomposition, Version 1

Suppose a  $\Gamma$ -periodic (Hamilton) integral operator

$$H_0 : \ell^2(\Lambda) \rightarrow \ell^2(\Lambda), \quad (2.9)$$

is given. We define  $\Gamma$ -periodicity to mean that that the integral kernel of  $H_0$  satisfies

$$H_0(x, y) := \langle \delta_x, H_0 \delta_y \rangle = H_0(x + \gamma, y + \gamma) \quad (x, y \in \Lambda, \quad \forall \gamma \in \Gamma).$$

The periodicity allows for Bloch-Floquet decomposition;  $\ell^2(\Lambda)$  is unitarily equivalent with the constant fiber Hilbert space  $\int_{\Omega^*}^{\oplus} \mathbb{C}^2 dk$  by a unitary operator, which is the extension of  $\tilde{U} : \ell_c^2 \rightarrow \int_{\Omega^*}^{\oplus} \mathbb{C}^2 dk$  defined by

$$(\tilde{U}\psi)(k; \underline{x}) := \frac{1}{\sqrt{|\Omega^*|}} \sum_{\gamma \in \Gamma} e^{-ik \cdot \gamma} \psi(\gamma + \underline{x}) \quad (\psi \in \ell_c^2(\Lambda), k \in \Omega^*, \underline{x} \in \mathcal{B}). \quad (2.10a)$$

where every  $f(k)$  in the fiber spaces  $\mathbb{C}^2$ ,  $k \in \Omega^*$  has the form

$$f(k) = \begin{bmatrix} f(k; \underline{\xi}) \\ f(k; \underline{\zeta}) \end{bmatrix}$$

Note that we use  $\tilde{U}$  for the extension of  $\tilde{U}$  also. The variable  $k$  is often called the crystal-momentum or quasi-momentum.  $H_0$  is a fibered operator  $\tilde{U}H_0\tilde{U}^* = \int_{\Omega^*} \tilde{h}_0(k) dk$  with fibers  $\tilde{h}_0(k) = \begin{bmatrix} \tilde{h}_0(k; \underline{\xi}, \underline{\xi}) & \tilde{h}_0(k; \underline{\xi}, \underline{\zeta}) \\ \tilde{h}_0(k; \underline{\zeta}, \underline{\xi}) & \tilde{h}_0(k; \underline{\zeta}, \underline{\zeta}) \end{bmatrix}$  satisfying

$$\begin{aligned} H_0(\gamma + \underline{x}, \underline{x}') &= \frac{1}{|\Omega^*|} \int_{\Omega^*} dk e^{ik\cdot\gamma} \tilde{h}_0(k; \underline{x}, \underline{x}') \quad (\underline{x}, \underline{x}' \in \mathcal{B}; \gamma \in \Gamma), \\ \tilde{h}_0(k; \underline{x}, \underline{x}') &= \sum_{\gamma \in \Gamma} e^{-ik\cdot\gamma} H_0(\underline{x} + \gamma, \underline{x}') \quad (\underline{x}, \underline{x}' \in \mathcal{B}; k \in \Omega^*). \end{aligned} \tag{2.10b}$$

The main result of this article concerns two isolated energy bands touching in “Dirac”-cones, for instance, when  $\Lambda$  is the honeycomb lattice (graphene), and  $H_0$  is a tight-binding Hamiltonian. We briefly remind the reader of a nearest-neighbour tight-binding calculation of the graphene band structure, not essentially different from the one presented in [13]. The nearest-neighbour tight-binding band structure is one the simplest band structure calculations for graphene. Note that the Dirac-cones is a general artifact of the honeycomb lattice, not a property of the nearest-neighbour tight-binding approximations, see [4].

### 2.3. A Calculation of the Energy Spectrum of Graphene

First, fix the length-scale such that the nearest-neighbour distance is 1. For graphene a standard choice of Bravais lattice is  $\mathbf{a} = \frac{1}{2}(\sqrt{3}, 3)$ ,  $\mathbf{b} = \frac{1}{2}(-\sqrt{3}, 3)$ , see Fig. 1, leading to the dual lattice vectors  $\mathbf{a}^* = 2\pi(\frac{1}{\sqrt{3}}, \frac{1}{3})$ ,  $\mathbf{b}^* = 2\pi(-\frac{1}{\sqrt{3}}, \frac{1}{3})$ . We choose the

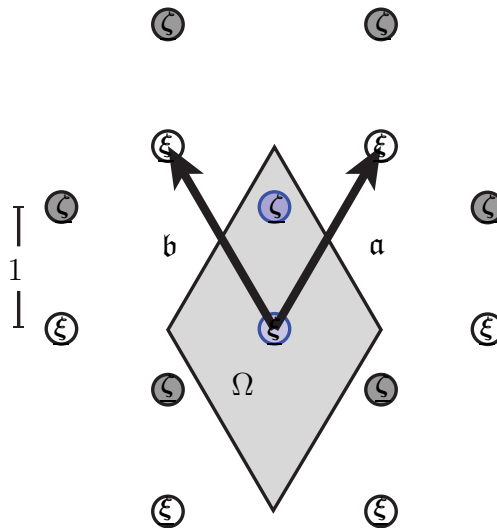


Fig. 1. Graphene crystal structure. The vectors  $\mathbf{a}$  and  $\mathbf{b}$  generates the Bravais lattice  $\Gamma$ . We choose the length-scale such that the nearest neighbour distance is 1.

graphene basis, see Fig. 1,

$$\mathcal{B}^G = \{(0, 0), (0, 1)\}. \tag{2.11}$$

A simple discrete Hamiltonian for graphene is the often used nearest-neighbour model:

$$H_0^G(x, x') = \begin{cases} 1 & \text{if } \|x - x'\| = 1, \\ 0 & \text{if } \|x - x'\| \neq 1 \end{cases} \quad (x, x' \in \Lambda). \quad (2.12)$$

In this model, the fiber matrix, found by inserting (2.11) and (2.12) into formula (2.10b) is

$$\tilde{h}_0^G(k) = \begin{bmatrix} 0 & 2e^{-i\frac{3}{2}k_2} \cos\left(\frac{\sqrt{3}}{2}k_1\right) + 1 \\ 2e^{i\frac{3}{2}k_2} \cos\left(\frac{\sqrt{3}}{2}k_1\right) + 1 & 0 \end{bmatrix} \quad (2.13)$$

and the famous band functions are given by the eigenvalues of (2.13) as function of  $k = (k_1, k_2) \in \Omega^*$ :

$$\begin{aligned} \lambda_1(k_1, k_2) &= -\sqrt{3 + 2 \cos(\sqrt{3}k_2) + 4 \cos\left(\frac{\sqrt{3}}{2}k_2\right) \cos\left(\frac{3}{2}k_1\right)}, \\ \lambda_2(k_1, k_2) &= \sqrt{3 + 2 \cos(\sqrt{3}k_2) + 4 \cos\left(\frac{\sqrt{3}}{2}k_2\right) \cos\left(\frac{3}{2}k_1\right)}, \end{aligned} \quad (2.14)$$

plotted in Fig. 2. At the Dirac points

$$K_{\pm} = \left( \pm \frac{2\pi}{3}, \frac{2\pi}{3\sqrt{3}} \right) \quad (2.15)$$

see Fig. 2, the bands touch;  $\lambda_1(K_{\pm}) = \lambda_2(K_{\pm}) = 0$ . All other values of  $k$  where  $\lambda_1(k) \geq 0$ , or  $\lambda_2(k) \leq 0$  can be reached by adding integer multiples of  $\mathbf{a}^*$  and  $\mathbf{b}^*$  to  $K_{\pm}$ . In this sense  $K_{\pm}$  are the only distinct zeros of  $\lambda_{\nu}$ ,  $\nu = 1, 2$ . By symmetry of the two energy bands and half-filling,  $\lambda_1(K_{\pm}) = \lambda_2(K_{\pm}) = 0$  is also the Fermi energy for this model, and the Fermi surface consists of isolated points.

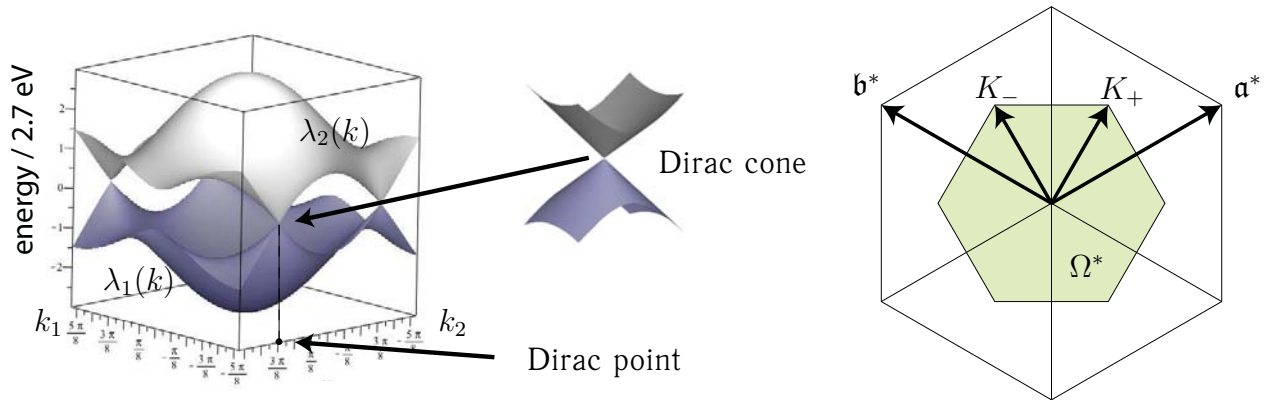


Fig. 2. Electron-energies of isolated graphene as a function of the crystal momentum  $k \in \Omega^*$  (in units of the nearest neighbour hopping constant  $\sim 2,7eV$ ). Of special interest are the “Dirac” points,  $K$ , where the two bands touch conically.

When expanding the fiber component functions  $h_0^G(\cdot; \underline{x}, \underline{x}')$ ,  $\underline{x}, \underline{x}' \in \mathcal{B}$  around  $K_+$ , one gets

$$h_0^G(\tilde{k}_1, \tilde{k}_2) = \frac{3}{2} \begin{bmatrix} 0 & \tilde{k}_1 - i\tilde{k}_2 + \sum_{|\alpha| \geq 2} C_\alpha \tilde{k}^\alpha \\ \tilde{k}_1 + i\tilde{k}_2 + \dots & 0 \end{bmatrix}, \quad \tilde{k} = k - K_+.$$

which to first order in  $k_1$  and  $k_2$  is the fiber of the Dirac Hamiltonian for massless fermions, also known as the *Weyl Hamiltonian*.

**2.3.1. The uniform external magnetic field.** Now consider a general one-electron Hilbert space  $\ell^2(\Lambda)$ , where  $\Lambda$  is a crystal structure of atom-sites in the  $XY$ -plane.

An uniform orthogonal magnetic field  $B$  is incorporated into the model by Peierls substitution [6, 8, 11]; we thus define a magnetic Hamiltonian with the integral kernel

$$H_b(\gamma + \underline{x}, \gamma' + \underline{x}') := e^{iB(\gamma_1\gamma'_2 - \gamma_2\gamma'_1)} H_0(\gamma + \underline{x}, \gamma' + \underline{x}') \quad (\gamma, \gamma' \in \Gamma, \quad \underline{x}, \underline{x}' \in \mathcal{B}), \quad (2.16)$$

where  $B(\gamma_1\gamma'_2 - \gamma_2\gamma'_1)$  is the flux of the magnetic field  $B$  through the triangle generated by origin,  $\gamma$  and  $\gamma'$ .

**2.3.2. Bloch-Floquet decomposition, version 2.** It is convenient to introduce an operator  $U$  defined on  $\ell^2(\Lambda)$  by extension of

$$(U\psi)(k, \underline{x}) := \frac{1}{\sqrt{|\Omega^*|}} \sum_{\gamma \in \Gamma} e^{-ik \cdot (\gamma + \underline{x})} \psi(\gamma + \underline{x}) \quad (\psi \in \ell^2_c(\Lambda), \quad k \in \Omega^*, \quad \underline{x} \in \mathcal{B}) \quad (2.17)$$

(compare with (2.10).)  $U$  associates a vector  $\psi \in \ell^2(\Lambda)$  with a vector  $U\psi \in \int_{\Omega^*}^{\oplus} \mathbb{C}^2 dk$ . The crystal Hamiltonian is again unitarily equivalent with a fibered operator acting in  $\int_{\Omega^*}^{\oplus} \mathbb{C}^2 dk$ :

$$UH_0U^* = \int_{\Omega^*}^{\otimes} dk h_0(k), \quad (2.18)$$

where each fiber can be represented as a self-adjoint  $2 \times 2$  matrix

$$h_0(k) = \begin{bmatrix} h_0(k; \underline{\xi}, \underline{\xi}) & h_0(k; \underline{\xi}, \underline{\zeta}) \\ h_0(k; \underline{\zeta}, \underline{\xi}) & h_0(k; \underline{\zeta}, \underline{\zeta}) \end{bmatrix} \quad (\mathcal{B} = \{\underline{\xi}, \underline{\zeta}\}). \quad (2.19)$$

The unitary  $U$  fixes the integral kernel of the fibers  $h_0(k)$  from the kernel of  $H_0$ , and vice versa:

$$h_0(k; \underline{x}, \underline{x}') = \frac{1}{|\Omega^*|} \sum_{\gamma \in \Gamma} e^{-ik \cdot (\underline{x} + \gamma - \underline{x}')} H_0(\underline{x} + \gamma, \underline{x}') \quad (k \in \Omega^*, \quad \underline{x}, \underline{x}' \in \mathcal{B}), \quad (2.20a)$$

$$H_0(x, x') = \frac{1}{|\Omega^*|} \int_{\Omega^*} dk e^{ik \cdot (x - x')} h_0(k; \underline{x}, \underline{x}') \quad (x = \underline{x} + \gamma \in \Lambda, \quad x' = \underline{x}' + \gamma' \in \Lambda). \quad (2.20b)$$

## 2.4. The Main Result

We will now consider a simpler situation than graphene. We suppose that the fibered zero-field Hamiltonian has a dispersion relation with a single Dirac-cone situated at the origin.

**Theorem 2.1.** *Let  $\mathcal{L}(\mathbb{C}^2)$  denote the space of  $2 \times 2$  matrices with complex components. Consider a matrix valued mapping  $h_0 : \mathbb{R}^2 \supset \Omega^* \rightarrow \mathcal{L}(\mathbb{C}^2)$ , where  $h_0(k)$  is self-adjoint for all  $k$ . Let  $H_0 : \ell^2(\Lambda) \rightarrow \ell^2(\Lambda)$  be a zero-field crystal Hamiltonian generated by  $h_0$  by (2.19) and (2.20b). Furthermore assume that*

- (a): for fixed  $\underline{x}, \underline{x}' \in \mathcal{B}$ , the function  $\Omega^* \ni k \mapsto e^{ik \cdot (\underline{x} - \underline{x}')} h_0(k; \underline{x}, \underline{x}') \in \mathbb{C}$  has an extension which is  $C^\infty(\mathbb{R}^2)$  and  $\Gamma^*$ -periodic;
- (b): 0 is an eigenvalue of  $h_0(0)$  with degeneracy 2;
- (c): for  $k \neq 0$ ,  $h_0(k)$  has two distinct eigenvalues  $\lambda_1(k) < 0 < \lambda_2(k)$ ;

(d):  $h_0(k) = h_0^{[1]}(k) + h_0^{Rem}(k)$ , where

$$h_0^{[1]}(k_1, k_2) = \begin{bmatrix} 0 & k_1 - ik_2 \\ k_1 + ik_2 & 0 \end{bmatrix}, \tag{2.21}$$

and that there exists a constant  $C_1 > 0$  such that

$$\|h_0^{Rem}(k)\| \leq C_1 \|k\|^2 \quad (k \in \Omega^*). \tag{2.22}$$

Then the spectrum of the magnetic Hamiltonian  $H_b : \ell^2(\Lambda) \rightarrow \ell^2(\Lambda)$ , defined by (2.20b) and (2.16) above, develops gaps proportional to  $\sqrt{b}$  around the origin. To be precise: for fixed  $M = 0, 1, 2, 3, \dots$ , choose  $c_1, c_2$  such that

$$\sqrt{2M} < c_1 < c_2 < \sqrt{2(M+1)}. \tag{2.23}$$

Then there exists  $b_0 > 0$  such that for all  $0 < b < b_0$  we have

$$[c_1\sqrt{b}, c_2\sqrt{b}] \subset \rho(H_b). \tag{2.24}$$

(see Fig. 3).

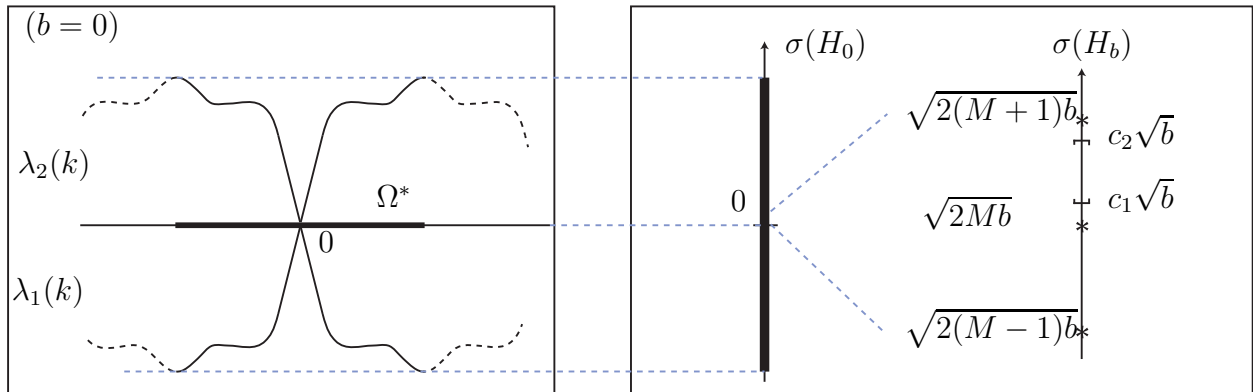


Fig. 3. *Left:* The two energy band functions  $\lambda_1$  and  $\lambda_2$ , in the zero field case, qualitatively sketched (in reality, the functions are real-valued functions on  $\Omega^* \subset \mathbb{R}^2$ , of the type like Fig. 2, but only with one Dirac point at the origin). *Right:* The energy spectrum in two situations; no external magnetic field  $b = 0$  (left vertical axis, a continuous energy band), and constant external magnetic field,  $b > 0$  (right vertical axis). Gaps  $[c_1\sqrt{b}, c_2\sqrt{b}]$  between the low Landau levels  $\sqrt{2Mb}$ ,  $M = 0, 1, 2, \dots$  (marked by stars) appear in the spectrum of  $H_b$  when  $b$  is sufficiently small but non-zero.  $\sqrt{2M} < c_1 < c_2 < \sqrt{2(M+1)}$  for some  $M \in \mathbb{N}_0$  small enough. Note that the right vertical axis only covers a tiny portion of the energy values which are inside the zero-field energy band, the two vertical axis are not of same scale!

### 2.5. About the Proof

Full proofs will be given in another paper of M. H. Brynildsen, H. D. Cornean, and I. Herbst. We construct an approximation for  $(H_b - z)^{-1}$ , using a cut-and-paste method. The main idea is to treat fibers  $h_0(k)$ , with  $k$  near the Dirac points, with the continuous Dirac-resolvent, this is where the Landau levels come into play. The proof heavily relies on the  $\sqrt{B}$ -behaviour of the Hausdorff distance between spectra of Hamiltonians which differ only by a Peierls phase, as proven in [2].

### 3. Conclusions

Our result can be extended to the double-cone situation. The fact that there are gaps near the Dirac points is in agreement with the numerical calculations of Hofstadter-type [5], which were applied to the honeycomb-lattice in [12] and expanded in [3]. They plot the spectrum for values of  $B$  for which the relative flux of the external magnetic field through one unit cell has rational values.

For small intensities of the external magnetic field the Hofstadter-Rammal plot becomes increasingly computationally heavy to produce, so the more modern articles with better access to computer-power have extended the “Hofstadter-Rammal butterfly” spectrum plot to lower field-strengths (compare, for instance, our result with [3, Fig. 2a]).

Our method does not distinguish between rational or irrational fluxes, since we do not concern ourselves with the nature of the spectrum, we only want to show the existence of gaps in the spectrum. Also, our result holds for all  $B$  in a small neighborhood of zero, whereas the Hofstadter approach requires more computations, the smaller  $B$  is.

### 4. Acknowledgments

The authors acknowledge partial support from the Danish FNU grant *Mathematical Analysis of Many-Body Quantum Systems*. The authors wish to thank the organizers of the conference *Mathematical Challenge of Quantum Transport in Nanosystems, St. Petersburg, 2013*.

### References

- [1] A. H. Castro Neto, F. Guinea, N. M. R. Peres, K. S. Novoselov, and A. K. Geim. The electronic properties of graphene. *Reviews of Modern Physics*, **81**, P. 109–162 (2009).
- [2] H. D. Cornean, R. Purice. On the regularity of the Hausdorff distance between spectra of perturbed magnetic Hamiltonians. *Spectral Analysis of Quantum Hamiltonians*, P. 55–66 (2012).
- [3] P. Dietl, F. Piéchon, and G. Montambaux. New magnetic field dependence of Landau levels in a graphenelike structure. *Physical review letters*, **100** (23), P. 236405 (2008).
- [4] C. L. Fefferman, M. I. Weinstein. Honeycomb lattice potentials and Dirac points. *J. Amer. Math. Soc.*, **25**, P. 1169–1220 (2012).
- [5] D. R. Hofstadter. Energy levels and wave functions of Bloch electrons in rational and irrational magnetic fields. *Physical review B*, **14** (6), P. 2239 (1976).
- [6] J. M. Luttinger. The effect of a magnetic field on electrons in a periodic potential. *Phys. Rev.*, **84** (4) P. 814–817 (1951).
- [7] G. Nenciu. Bloch electrons in a magnetic field: Rigorous justification of the Peierls-Onsager effective Hamiltonian. *Letters in mathematical physics*, **17** (3), P. 247–252 (1989).
- [8] G. Nenciu. Dynamics of band electrons in electric and magnetic fields: rigorous justification of the effective Hamiltonians. *Rev. Mod. Phys.*, **63** (1), P. 91–127 (1991).
- [9] K. S. Novoselov, A. K. Geim, et al. Two-dimensional gas of massless Dirac fermions in graphene. *Nature*, **438** (7065), P. 197–200 (2005).
- [10] K. S. Novoselov, A. K. Geim, et al. Electric field effect in atomically thin carbon films. *Science*, **306** (5696), P. 666–669 (2004).
- [11] R. Peierls. Zur theorie des diamagnetismus von leitungselektronen. *Zeitschrift für Physik A Hadrons and Nuclei*, **80** (11), P. 763–791 (1933).
- [12] R. Rammal. Landau level spectrum of Bloch electrons in a honeycomb lattice. *Journal de Physique*, **46** (8), P. 1345–1354 (1985).
- [13] P. R. Wallace. The band theory of graphite. *Physical Review*, **71** (9), P. 622 (1947).